On the Dynamics of a Cavitating Pump

Christopher Earls Brennen
California Institute of Technology, Pasadena, California 91125, USA
E-mail: brennen@caltech.edu

Abstract. This paper presents a review of some of the recent developments in our understanding of the dynamics and instabilities caused by cavitation in pumps. Focus is placed on presently available data for the transfer functions for cavitating pumps and inducers, particularly on the compliance and mass flow gain factor which are so critical for pump and system stability. The resonant frequency for cavitating pumps is introduced and contexted. Finally emphasis is placed on the paucity of our understanding of pump dynamics when the device or system is subjected to global oscillation.

1. Introduction

Since the first experimental measurements many years ago of the complete dynamic transfer function for a cavitating pump [1,2] there has been a general recognition of the importance of various components of these transfer functions (particularly the cavitation compliance and mass flow gain factor) in determining the dynamic characteristics and instabilities of systems incorporating such pumps (see for example [3,4,5,6,7]). The present paper attempts to summarize some of the recent understandings and to evaluate the current state of knowledge of transfer functions for cavitating pumps.

2. Pump Transfer Function Data

The linear dynamic transfer matrix for a pump is denoted here by TP_{ij} and is defined by

$$\begin{Bmatrix} P_2 \\ m_2 \end{Bmatrix} = \begin{bmatrix} TP_{11}\, TP_{12} \\ TP_{21}\, TP_{22} \end{bmatrix} \begin{Bmatrix} P_1 \\ m_1 \end{Bmatrix} \tag{1}$$

where P and m are the complex, linearized fluctuating total pressure and mass flow rate and subscripts 1 and 2 refer to the pump inlet and discharge respectively. In general TP_{ij} will be a function of the frequency, ω, of the perturbations and the mean flow conditions in the pump including the design, the cavitation number, σ, and the flow coefficient. In this review we will focus primarily on the second of these equations and on TP_{21} and TP_{22} since cavitation has a major effect on these characteristics and they therefore have a critical influence on the potential instabilities in the fluid system in which the pump is installed. But it is valuable in passing to note that $TP_{12} = -R - j\omega L$ where R is the pump resistance and L is the pump inertance (valuable measurements of these dynamic characteristics for a non-cavitating pump were first made by Ohashi [8] and by Anderson *et al.* [9]). In the absence of cavitation and compressibility effects $TP_{11} = 1$ but its departure from unity due to cavitation is also important in pump dynamics.

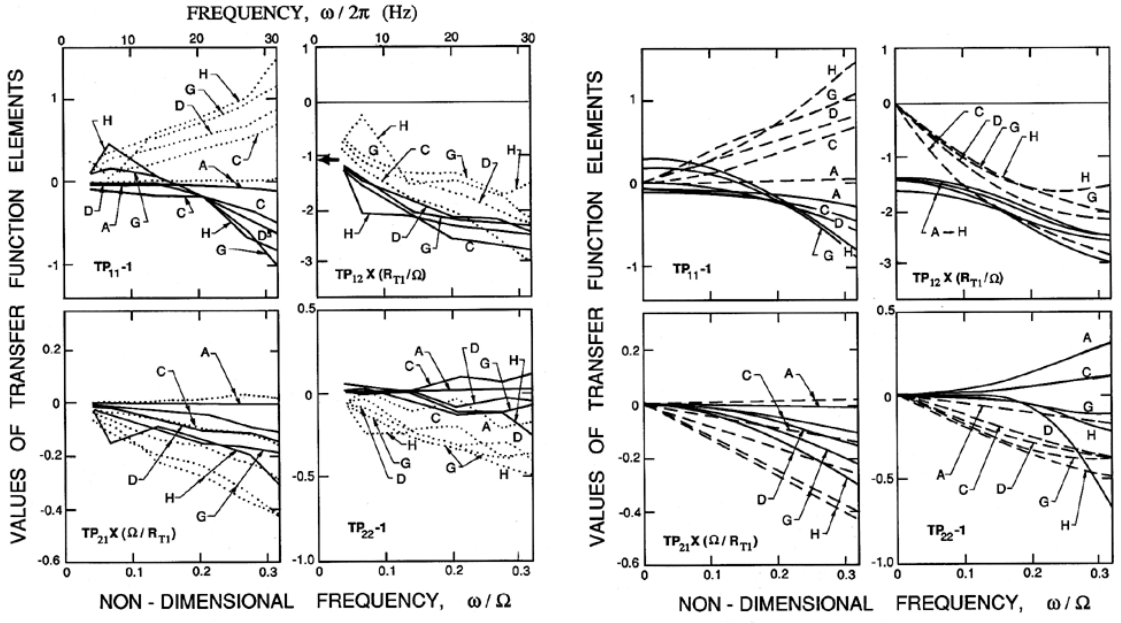

Figure 1. Left: Typical transfer functions for a cavitating inducer obtained by Brennen [2] for the 10.2 *cm* diameter SSME inducer operating in water at 6000 *rpm* and a flow coefficient of $\phi_1 = 0.07$. Data is shown for four different cavitation numbers, σ = (A) 0.37, (C) 0.10, (D) 0.069, (G) 0.052 and (H) 0.044. Real and imaginary parts are denoted by the solid and dashed lines respectively. The quasistatic pump resistance is indicated by the arrow. Right: Polynomial curves fitted to the data on the left. Adapted from Brennen [2].

The transfer function and other pump dynamic characteristics presented in this paper are non-dimensionalized in the manner of Brennen *et al.* [2]. Specifically the frequency, ω, is non-dimensionalized as $\omega' = \omega h/U_t$ where h is the peripheral blade tip spacing at the inlet to the pump or inducer ($h = 2\pi R_t/N$ where R_t is the inlet tip radius and N is the number of main blades) and U_t is the inlet tip speed ($U_t = \Omega R_t$ where Ω is the rotational speed in *rad/s*). Then the compliance, C, and mass flow gain factor, M, are defined by expanding the transfer function elements, TP_{21} and TP_{22}, at low frequency in power series in $j\omega$:

$$TP_{21} \;=\; -j\omega C \;+\; (j\omega)^2 C^* + \ldots \tag{2}$$

$$TP_{22} \;=\; 1 \;-\; j\omega M \;+\; (j\omega)^2 M^* + \ldots \tag{3}$$

The compliance, C, and mass flow gain factor, M, are non-dimensionalized by

$$\frac{CN\Omega^2}{4\pi^2 R_t} \quad \text{and} \quad \frac{MN\Omega}{2\pi} \tag{4}$$

Note that the above non-dimensionalization scheme differs from that used in Brennen [10] but is preferred since each blade produces cavitation that contributes to C and M.

Those first experimental measurements of the complete dynamic transfer function for a cavitating pump [1,2] were carried out in water with a series of model inducers including a scale model of the low pressure LOX inducer in the Space Shuttle Main Engine (SSME). Measured transfer functions for that 10.2*cm* diameter SSME inducer operating in water at 6000 *rpm*, a flow coefficient of $\phi_1 = 0.07$ and various cavitation numbers, σ, are reproduced in figure 1 (left)

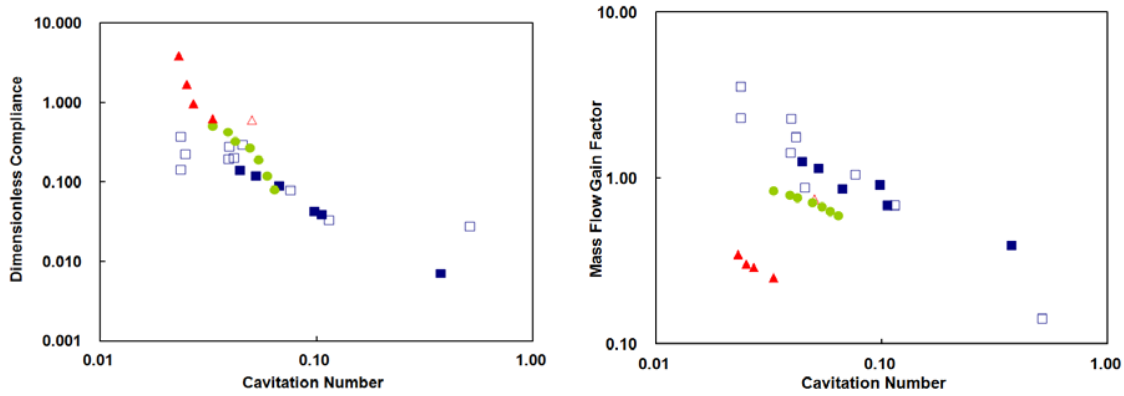

Figure 2. Dimensionless cavitation compliance (left) and mass flow gain factor (right) plotted against tip cavitation number for: [a] Brennen [2] SSME 10.2cm model inducer in water (solid blue squares) [b] Brennen [2] SSME 7.6cm model inducer in water (open blue squares) [c] Brennen & Acosta [11] J2-Oxidizer (solid green circles) analysis [d] Hori & Brennen [12] LE-7A LOX data (solid red triangles) [e] Shimura [13] LE-7 LN2 data (open red triangles).

where the four transfer functions elements are each plotted against a dimensionless frequency, the real parts as the solid lines and the imaginary parts as dashed lines. We should note that this data necessarily has substantial uncertainity associated with it and therefore polynomial fits in the Laplace variable $j\omega$ were produced in order to extract quantities like R, L, C and M (the polynomial fits to figure 1 (left) are shown on figure 1 (right)). A collection of the available data on the compliance and the mass flow gain factor is presented in figure 2 where those quantities are plotted against the cavitation number. The data on the SSME inducers in water is extracted from figure 1 while the J2 oxidizer data was derived by Brennen and Acosta [11] using test data and a heuristic dynamic model of the test facility. The LE-7 test data in liquid nitrogen was obtained by Shimura [13]. The LE-7A data is the only LOX data and was also extracted from test data by Hori and Brennen [12]. All of this data is subject to significant uncertainty though the original SSME data is probably the most reliable since it is based on measurements of the complete dynamic transfer function. Nevertheless, with one exception, both the compliance and mass flow gain factor data exhibit significant consistency in which both C and M are inversely proportional to σ. The exception is the LE-7A LOX data for the mass flow gain factor; whether this discrepancy is within the uncertainty band or an actual LOX thermal effect remains to be determined.

Before further discussion of this data collection we digress briefly to introduce a property in the dynamics of cavitating pumps that has not received sufficient attention in the past, namely the fundamental resonant frequency of a cavitating pump.

3. Resonant Frequency of a Cavitating Pump

It has been known for a long time that a cavitating inducer or pump may exhibit a violent surge oscillation at subsynchronous frequencies that results in very large pressure and flow rate oscillations in the system of which the pump is a part [14,15,16,17,18,10,19]. In the early days, this was known as "auto-oscillation" but the preferred name in recent times has been "cavitation surge". It typically occurs at low cavitation numbers just above those at which cavitation head loss becomes severe. Often it is preceded by a rotating cavitation pattern (see, for example, [20,21,22,19]). Figure 3 reproduces data on the frequencies of oscillation observed for the model SSME inducer and for a helical inducer by Braisted and Brennen [18]; they also plotted a rough

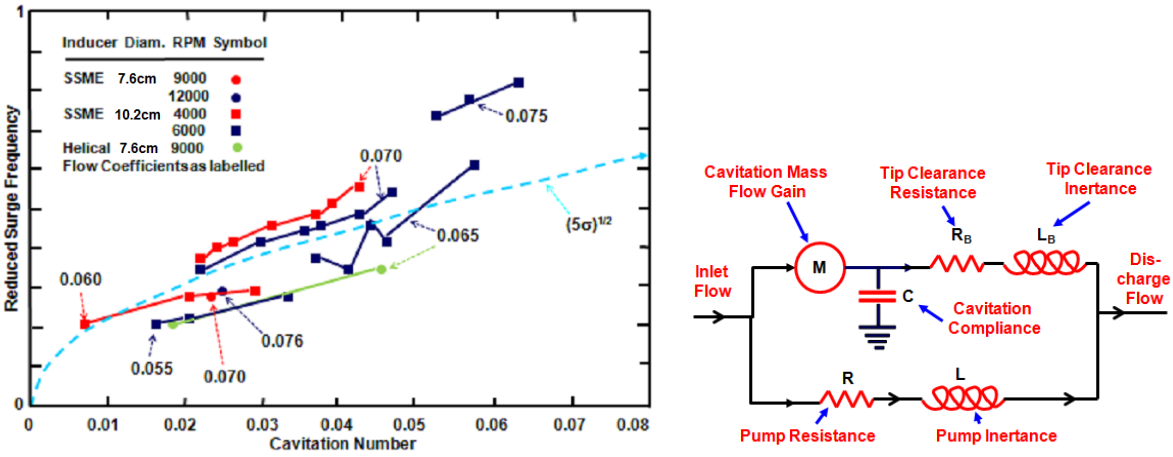

Figure 3. Left: Non-dimensional cavitation surge frequency as a function of cavitation number for the SSME model inducers at various speeds and flow coefficients as shown. The theoretical prediction is the dashed blue line, $(5\sigma)^{\frac{1}{2}}$. Adapted from from [18]. Right: A dynamic model of the main flow and the parallel tip clearance backflow in a cavitating inducer.

empirical fit to that data which approximated the dimensionless surge frequency by $(5\sigma)^{\frac{1}{2}}$. More recently we recognize that this "natural frequency of a cavitating pump" has a more fundamental origin as follows:

Almost any reasonable, proposed dynamic model for a cavitating inducer or pump (such as that on the right of figure 3 designed to simulate the parallel streams of main flow and tip clearance flow) which incorporates both the pump inertance, L, and the cavitation compliance, C, clearly exhibits a natural frequency, Ω_P, given by

$$\Omega_P \;=\; \frac{1}{(LC)^{\frac{1}{2}}} \tag{5}$$

Using the data for the SSME LOX inducer from [10] we can approximate L and C by

$$L \;\approx\; \frac{10}{R_t} \quad \text{and} \quad C \;\approx\; \frac{0.05 R_t}{\sigma \Omega^2} \tag{6}$$

so that, substituting into equation 5,

$$\frac{\Omega_P}{\Omega} \;\approx\; (2\sigma)^{\frac{1}{2}} \quad \text{or} \quad \Omega'_P \;\approx\; \frac{\Omega_P h}{U_t} \;\approx\; (5\sigma)^{\frac{1}{2}} \tag{7}$$

This is precisely the same as the result proposed empirically by Braisted and Brennen [10] and shown on the left in figure 3. We will refer to this as the natural frequency of a cavitating pump. Indeed the data of figure 3 displays further detail of this cavitating pump property. There is a manifest trend for the frequency to decrease somewhat with flow coefficient and this seems certain to be the result of an increasing volume of cavitation and increasing compliance as the blades are loaded up at lower flow coefficients. It is important to emphasize that this does not necessarily mean that the major system instability oscillations occur at this frequency. The study of Hori and Brennen [13] discussed later in this paper shows, however, that major instabilities or resonances can occur when this natural frequency for a cavitating pump coincides with other system frequencies such as an organ pipe mode in a suction or discharge tube.

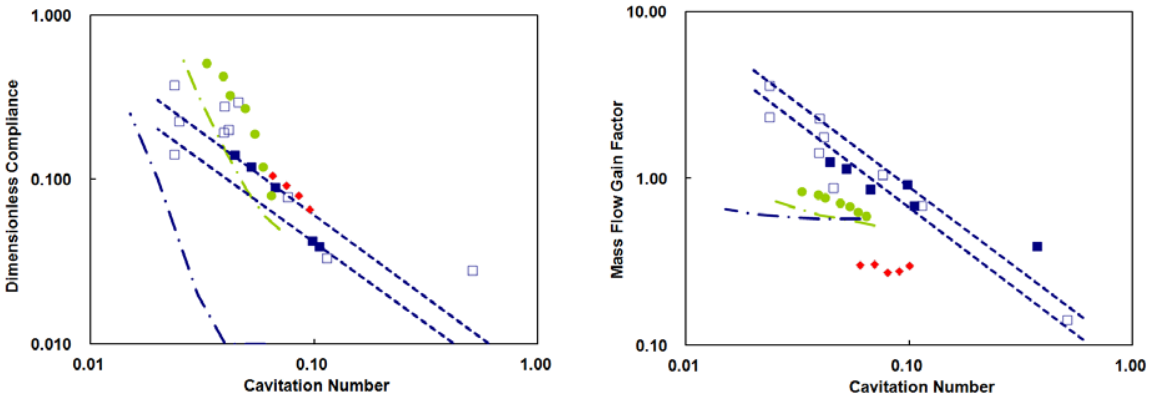

Figure 4. Dimensionless cavitation compliance (left) and mass flow gain factor (right) plotted against tip cavitation number for: [a] Brennen *et al.* [2] SSME 10.2cm model inducer in water (solid blue squares) [b] Brennen *et al.* [2] SSME 7.6cm model inducer in water (open blue squares) [c] Brennen [24] bubbly flow model results (dashed blue lines) [d] Brennen & Acosta [11] SSME LPOTP blade cavitation prediction (dot-dash blue line) [e] Brennen & Acosta [11] J2-Oxidizer data (solid green circles) [f] Brennen & Acosta [11] J2-Oxidizer blade cavitation prediction (dot-dash green line) [g] Yonezawa *et al.* [25] quasistatic CFD cascade data (solid red diamonds).

4. Comments on some analytical models

We comment in the conclusions on the difficulties with any detailed CFD approach that aims to predict the dynamic transfer function for a cavitating inducer. It seems clear that much progress in developing reduced order models for cavitation in the complex geometry of an inducer (and, in particular, for the backflow cavitation) will be needed before this approach will provided practical and useful guidance. However, in the short term crude, one-dimensional models and lumped parameter models (see, for example, Cervone *et al.* [23]) guided by the existing data base can give useful benchmarks. The bubbly flow model of Brennen [24] incorporated several of the basic phenomena that we now know are inherent in the dynamic response of an inducer or pump. In particular, the compliance of the bubbly stream within the flow (though the compressibility of that bubbly flow had to be represented by a empirical constant, K') and the magnitude of the void fraction fluctuations produced by the fluctuating angle of attack (represented by a second empirical factor of proportionality, M'). These two features respectively lead to dynamic waves and to kinematic waves in the bubbly blade passage flow. Even though the two constants K' and M' were empirically chosen, typical transfer functions derived from the bubbly flow model showed encouraging similarity with the experimental transfer functions. The measured compliances and mass flow gain factors for the SSME inducers and for the J2 oxidizer inducer are reproduced in Figure 4 in order to compare that data with several predictions from the bubbly flow model (dashed blue lines for several choices of K' and M'). The predictions appear to provide a useful benchmark for future data evaluation and comparison.

Figure 4 also includes predictions from the blade cavitation analysis presented earlier by Brennen and Acosta [11]. That analysis has the advantage that it does not contain any empirical parameter, as such. However, it assumes that all the cavitation is contained within a single cavity attached to each blade. Moreover the comparisons in figure 4 suggest that such a model does not yield very useful results which is not surprising when photographs of practical inducers show that the cavitation is primarily bubbly cavitation and not blade cavitation (Brennen 1994).

Also included in figure 4 are some quasistatic compliances and mass flow gain factors very

recently derived by Yonezawa *et al* [25] from steady CFD calculations of the cavitating flow in linear cascades. They have also performed calculations at a series of flow coefficients that show a general trend of increasing compliance and mass flow gain factor as the flow coefficient is decreased.

5. Resonances in Globally Oscillating systems

The research literature clearly exhibits a strong bias toward investigations of flow instabilities in systems which are essentially at rest, usually in a research laboratory test stand. While this bias is understandable, it can be misleading for it tends to mask the difference between such a flow instability and the resonant response in a flow system subject to global fluctuation. This is particularly an issue with launch vehicle propulsion systems for they can exhibit some serious resonances with the oscillating vehicle structure. Following the approach originally developed by Rubin [3], Hori and Brennen [12] recently constructed a time-domain model for prototypical pumping systems in order to examine the response of those systems to globally imposed acceleration. They constructed dynamic models for four different configurations used during the testing and deployment of the LOX turbopump for the Japanese LE-7A rocket engine. As sketched in figure 5, these configurations include three ground-based facilities, two cold-test facilities (one with a suction line accumulator and the other without), and a hot-fire engine test facility. The fourth configuration is the flight hardware. All four configurations include the same LE-7A turbopump whose cavitation compliance and mass flow gain factor were extracted from the ground tests and were included in figure 2. The dynamic model for these LE-7A turbopump systems incorporated the time domain equivalent of the pump transfer function including pump cavitation compliance and mass flow gain factor terms as well as the known steady pump performance characteristic. It also included lumped parameter models for the storage tank (fuel or oxidizer), the accumulator, and the valves, as well as compressible, frictional flow equations for the flows in the feedlines. The assumed boundary conditions at inlet to and discharge from these hydraulic systems were an assumed storage tank pressure and the back

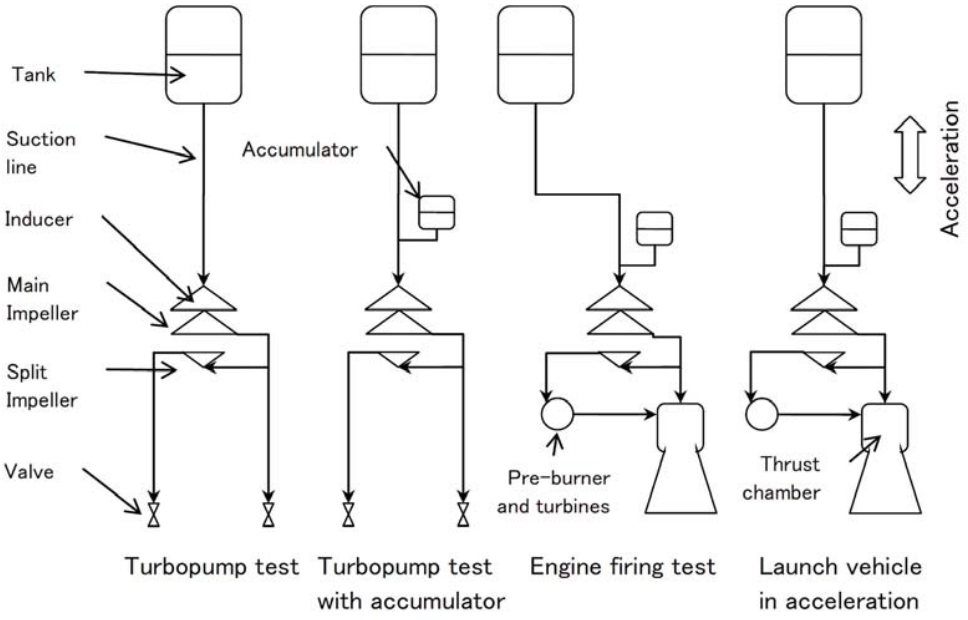

Figure 5. The four hydraulic system configurations whose dynamic responses are compared.

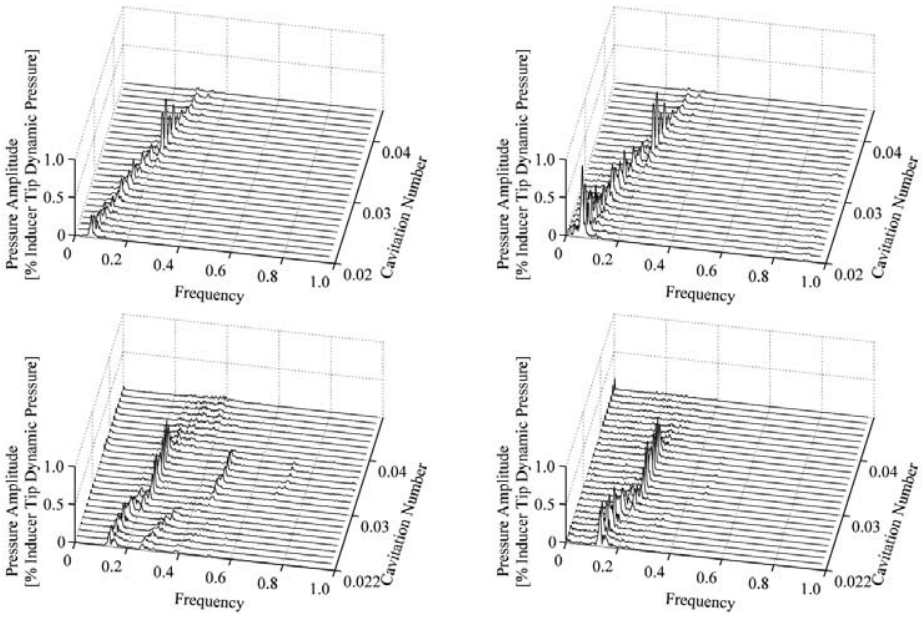

Figure 6. Model calculations (upper graphs) and test facility measurements (lower graphs) of the pump inlet pressure (left) and the inducer discharge pressure (right) from the cold test facility with an accumulator, the second configuration of Figure 5.

pressure in the combustion chamber or catchment tank. Additional, pseudo-pressure terms [26] were included in the flight configuration to account for the globally-imposed acceleration. These model equations were solved numerically in the time domain using the traditional methods of fluid transients [27,10] including the method of characteristics for the feedlines. Low-level white noise pressure perturbations were injected at the pump inlet in order to provide a trigger for potential cavitation surge, should that be inclined to occur. This technique is based on the assumption that the cavitation surge (and other dynamic responses) observed in the ground-based tests are similarly triggered by random pressure noise. We summarize here the key results that Hori and Brennen [12] obtained from the modeling of the four LE-7A test systems and the comparison of the models results with measurements of the pressure spectra obtained during tests of those systems.

The calculated and measured spectra for the three ground-based systems were quite similar and showed excellent agreement with the measurements. For a cavitation number greater than 0.04, the pressure fluctuations were very small indeed. However, when the cavitation number was decreased to a value of about 0.035, pressure fluctuations at a non-dimensional frequency of 0.22 became dominant as exemplified by the spectra shown in Figure 6 for the second configuration of Figure 5. This non-dimensional frequency of 0.22 is the afore-mentioned natural frequency of the cavitating pump and the increase in the response occurs when there is a resonance between that natural frequency (which decreases as σ decreases) and an organ pipe mode of oscillation of the suction line. The corresponding experimental spectra exhibit good qualitative agreement with the model calculations. However it is important to note that both the tests and the calculations exhibit very small pressure oscillation amplitudes, less than 1% of inducer tip dynamic pressure and this magnitude is inconsequential.

Hori and Brennen [12] then turned to the flight configuration. First the response of the flight configuration **without** imposed acceleration was investigated and only very small pressure oscillations (less than 0.01% of inducer tip dynamic pressure) and flow rate oscillations (less

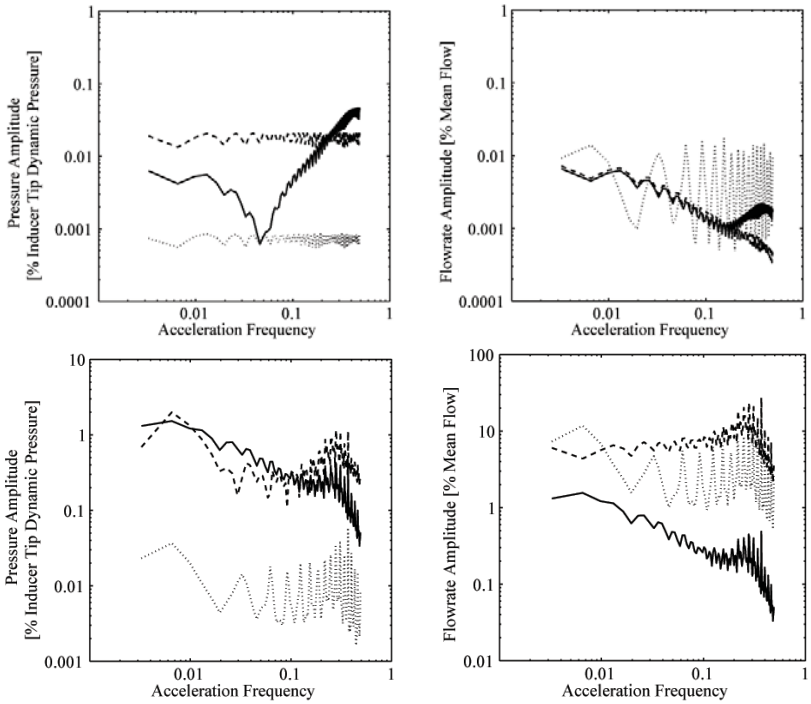

Figure 7. Model calculations for the flight configuration subject to global acceleration. Upper graphs: in the absence of pump cavitation. Lower graphs: when the pump cavitation number is $\sigma = 0.02$. Pressure amplitudes (left) and flow rate amplitudes (right) over a wide range of different oscillation frequencies and an oscillating acceleration magnitude of 0.1 m/s^2. Solid, dashed and dotted lines respectively present the pump discharge, inducer inlet and tank outlet quantities.

than 0.01% of mean flow) were calculated. Thus, like the first three configurations, the flight configuration is very stable in a non-accelerating frame. Then the model was used to examine the response of the flight configuration in a sinusoidally accelerating frame with an acceleration amplitude of 0.1 m/s^2 at various non-dimensional frequencies ranging from 0 to 0.5. The magnitude 0.1 m/s^2 would be characterisitic of the background excitation experienced in the rocket environment. Typical model results under non-cavitating conditions are shown in the upper graphs of figure 7 and are similar in magnitude to the results for the ground-based calculations; the conclusion is that, in the absence of cavitation, the system response is quite muted with pressure oscillation magnitudes less than 0.05% of inducer tip dynamic pressure and flow rate oscillation magnitudes less than 0.02% of mean flow.

Finally Hori and Brennen [12] present their key result, namely the response of the flight configuration to the same range of global oscillation (an acceleration magnitude of 0.1 m/s^2 for a range of oscillation frequencies), when the pump is **cavitating**. The lower graphs of figure 7 present the results for the lowest cavitation number examined namely $\sigma = 0.02$. It is clear that the result is a violent resonant response with amplitudes about two orders of magnitude greater than in the absence of cavitation. The pressure oscillation magnitudes are more than 2% of inducer tip dynamic pressure and the flow rate oscillation magnitudes are more than 20% of mean flow. Under these cavitating conditions, the largest flow rate magnitudes occur between the accumulator and the inducer at all frequencies and the largest pressure amplitudes occur at the inducer discharge. Thus the flow rate oscillation between the accumulator and the inducer

dominates the overall response and excites the rest of the system like an oscillating piston. The suction line from the tank to the accumulator also plays a role, albeit a secondary role. When the frequency of the "piston" coincides with an organ pipe mode of the compressible liquid between the tank and the cavitating inducer the entire system exhibits a peak response and this happens at each of those organ pipe modes. There is also an important global response maximum near the natural frequency of the cavitating pump (0.3); at higher frequencies the response dies off rather rapidly.

Thus the model calculations demonstrate how a violent resonant response can occur in the accelerating flight environment when pump cavitation is present and that this response can occur even when all the ground tests (and the model flight calculations without cavitation) indicate a stable and well-behaved response. The difficulty of duplicating these adverse flight environments in any ground test - and therefore of examining such an adverse condition - makes accurate model calculations an almost essential design tool.

6. Concluding Remarks

In concluding this review we should remark that despite significant progress in understanding the dynamics of cavitation in pumps and inducers, there is much that remains to be accomplished before an adequate pump system design procedure is completed. It is, perhaps, most useful in these concluding remarks to identify some of the most glaring gaps in our knowledge.

In terms of accomplishments we do have a reasonable data base supporting our preliminary understanding of the scaling of the dynamic transfer function with pump size, pump rotating speed (admittedly within a fairly narrow speed range), cavitation number and flow coefficient. However, most of that data is in water at roughly normal temperatures. Therefore the first deficiency is the lack of experimental data for the thermal effects on the dynamics. Thermal effects on cavitation and on the steady state performance of pumps have been extensively studied and are well known, for example, in the context of cryogenic pumps (see, for example, [10]); thermal effects in liquid oxygen are important and they are pervasive in liquid hydrogen pumps. But, apart from some preliminary tests [2,28,29] and some very limited theoretical considerations [30], little is really known about the thermal effects on the dynamic characteristics of cavitating pumps. Testing in fluids other than water is very limited though the recent work of Yoshida *et al.* [29] in liquid nitrogen suggests little thermal effect on cavitation surge. The lack of data is, in large measure, due to the absence of high fidelity dynamic flow meters for non-aqueous environments.

Another major gap in our current understanding has been evident for some time through the work of Rubin and others on the response of pump systems in globally oscillating environments and was particularly evident in the work of Hori and Brennen [12] described above. There are some very real questions about the dynamic response of cavitation and of cavitating pumps subjected to translational or rotational acceleration. The only surefire way to answer these questions is to conduct experiments with a pump loop experiment mounted on a shaker table that can impose substantial global oscillations up to frequencies of the order of $50Hz$ or more. Given the availability of huge shaker tables for earthquake engineering research and the known destructive consequences of instabilities such as the Pogo instability of liquid-propelled rockets, it is surprising that such experiments have not been carried out in the past.

Finally, I can anticipate that some will promote the use of computational models for cavitating flows in order to try to bridge these gaps. Though there have been some valuable efforts to develop CFD methods for cascades (see, for example, Iga *et al.*[31]), the problem with this suggestion is that accurate numerical treatments for cavitating pumps that will adequately represent both the non-equilibrium character of cavitation and adequately respond to flow fluctuations are still in a very early stage of development. Codes that can also handle the complex geometry and turbulence of the flow in an inducer including the tip clearance backflow

are many years away. It seems clear that much progress will be needed in the development of reduced-order models for cavitation before the computational approach can produce useful, practical results.

Acknowledgments
The author wishes to acknowledge the extensive and valuable support provided by the NASA George Marshall Space Flight Center, Huntsville, AL, during much of the research discussed in this paper. I also owe a great debt to my colleague and collaborator Allan Acosta as well as to numerous students at Caltech.

References

[1] Ng S L and Brennen C E 1978 *ASME J. Fluids Eng.* **100** 166-176
[2] Brennen C E, Meissner C, Lo E Y, and Hoffman G S 1982 *ASME J. Fluids Eng.* **104** 428-433
[3] Rubin S 1966 *AIAA J. Spacecraft and Rockets* **3** No.8 1188-1195
[4] Rubin S 1970 *Prevention of Coupled Structure-Propulsion Instability (POGO)* NASA Space Vehicle Design Criteria (Structures) NASA SP-8055
[5] Oppenheim B W and Rubin S 1993 *AIAA J. Spacecraft and Rockets* **30** No. 3 360-373
[6] Tsujimoto Y, Kamijo K and Brennen C 2001 *J. Propulsion and Power* **17** No.3 636-643
[7] Dotson K W, Rubin S and Sako B H 2005 *AIAA J. Propulsion and Power* **21** No.4 619-626
[8] Ohashi H 1968 *NASA TN D-4298*
[9] Anderson D A, Blade R J and Stevens W 1971 *NASA TN D-6556*
[10] Brennen C E 1994 *Hydrodynamics of Pumps* Oxford Univ. Press and Concepts ETI
[11] Brennen C E and Acosta A J 1976 *ASME J. Fluids Eng.* **98** 182-191
[12] Hori S and Brennen C E 2011 *J. Spacecraft and Rockets* **48** No.4 599-608
[13] Shimura T 1995 *AIAA J. Propulsion and Power* **11** No. 2 330-336
[14] Sack L E and Nottage H B 1965 *ASME J. Basic Eng.* **87** 917-924
[15] Rosenmann W 1965 *Proc. ASME Symp. on Cavitation in Fluid Machinery* 172-195
[16] Natanzon M S, Bl'tsev N E, Bazhanov V V, and Leydervarger M R 1974 *Fluid Mech. Soviet Res.* **3** No.1 38-45
[17] Miller C D and Gross L A 1967 *NASA TN D-3807*
[18] Braisted D M and Brennen C E 1980 *Polyphase Flow and Transport Technology* ed. R A Bajura, ASME Publ. New York 157-166
[19] Zoladz T 2000 *36th AIAA/ASME/SAE/ASEE Joint Propulsion Conf. AIAA-2000-3403, Huntsville, AL*
[20] Kamijo K, Shimura T and Tsujimoto Y 1994 *ASME Cavitation and Gas-Liquid Flow in Fluid Machinery and Devices* **190** 33-43
[21] Tsujimoto Y, Kamijo K and Yoshida Y 1993 *ASME J. Fluids Eng.* **115** No.1 135-141
[22] Hashimoto T, Yoshida M, Watanabe M, Kamijo K, and Tsujimoto Y 1997 *AIAA J. Propulsion and Power* **13** No. 4 488-494
[23] Cervone A, Tsujimoto Y, and Kawata Y 2009 *ASME J. Fluids Eng.* **131** No. 4
[24] Brennen C E 1978 *J. Fluid Mech.* **89** 223-240
[25] Yonezawa K, Aono J, Kang D, Horiguchi H, Kawata Y, and Tsujimoto Y 2012 Numerical Evaluation of Transfer Matrix of an Inducer under Cavitating Condition. Personal Communication.
[26] Batchelor G K 1967 *An Introduction to Fluid Dynamics* Cambridge Univ. Press
[27] Wylie E B, Streeter V L, and Suo L 1993 *Fluid Transients in Systems.* Prentice Hall.
[28] Yoshida Y, Sasao Y, and Watanabe M 2009 *ASME J. Fluids Eng.* **131** No.9 091302
[29] Yoshida Y Nanri H Kikuta K Kazami Y Iga Y and Ikohagi T 2011 *ASME J. Fluids Eng.* **133** No.6 061301
[30] Brennen C E 1973 *ASME J. Fluids Eng.* **95** 533-541
[31] Iga Y Nohmi M Goto A and Ikohagi T 2004 *ASME J. Fluids Eng.* **126** No.3 419-429